JOURNAL OF BACTERIOLOGY, Nov. 1998, p. 5828–5835 Vol. 180, No. 22
0021-9193/98/$04.00+0

Involvement of the Terminal Oxygenase β Subunit in the Biphenyl Dioxygenase Reactivity Pattern toward Chlorobiphenyls

YVES HURTUBISE, DIANE BARRIAULT, AND MICHEL SYLVESTRE*

Institut National de la Recherche Scientifique—Santé, Pointe-Claire, Québec, H9R 1G6 Canada

Received 22 May 1998/Accepted 3 September 1998

Biphenyl dioxygenase (BPH dox) oxidizes biphenyl on adjacent carbons to generate 2,3-dihydro-2,3-dihydroxybiphenyl in *Comamonas testosteroni* B-356 and in *Pseudomonas* sp. strain LB400. The enzyme comprises a two-subunit (α and β) iron sulfur protein (ISP_{BPH}), a ferredoxin (FER_{BPH}), and a ferredoxin reductase (RED_{BPH}). B-356 BPH dox preferentially catalyzes the oxidation of the double-*meta*-substituted congener 3,3′-dichlorobiphenyl over the double-*para*-substituted congener 4,4′-dichlorobiphenyl or the double-*ortho*-substituted congener 2,2′-dichlorobiphenyl. LB400 BPH dox shows a preference for 2,2′-dichlorobiphenyl, and in addition, unlike B-356 BPH dox, it can catalyze the oxidation of selected chlorobiphenyls such as 2,2′,5,5′-tetrachlorobiphenyl on adjacent *meta-para* carbons. In this work, we examine the reactivity pattern of BPH dox toward various chlorobiphenyls and its capacity to catalyze the *meta-para* dioxygenation of chimeric enzymes obtained by exchanging the ISP_{BPH} α or β subunit of strain B-356 for the corresponding subunit of strain LB400. These hybrid enzymes were purified by an affinity chromatography system as His-tagged proteins. Both types, the chimera with the α subunit of ISP_{BPH} of strain LB400 and the β subunit of ISP_{BPH} of strain B-356 (the $\alpha_{LB400}\beta_{B-356}$ chimera) and the $\alpha_{B-356}\beta_{LB400}$ chimera, were functional. Results with purified enzyme preparations showed for the first time that the ISP_{BPH} β subunit influences BPH dox's reactivity pattern toward chlorobiphenyls. Thus, if the α subunit were the sole determinant of the enzyme reactivity pattern, the $\alpha_{B-356}\beta_{LB400}$ chimera should have behaved like B-356 ISP_{BPH}; instead, its reactivity pattern toward the substrates tested was similar to that of LB400 ISP_{BPH}. On the other hand, the $\alpha_{LB400}\beta_{B-356}$ chimera showed features of both B-356 and LB400 ISP_{BPH} where the enzyme was able to metabolize 2,2′- and 3,3′-dichlorobiphenyl and where it was able to catalyze the *meta-para* oxygenation of 2,2′,5,5′-tetrachlorobiphenyl.

A fraction of the 209 polychlorinated-biphenyl (PCB) congeners can be transformed into chlorobenzoates by the bacterial biphenyl oxidative catabolic pathway. The pathway involves four enzymatic steps (9, 28). The biphenyl dioxygenase (BPH dox) catalyzes the first reaction of this pathway. Aromatic ring dioxygenases catalyze dihydroxylation reactions on two adjacent carbons of the aromatic ring (23). Some of these enzymes can oxygenate a broad range of substrate analogs. For example, naphthalene dioxygenase can catalyze the hydroxylation of several polycyclic aromatic hydrocarbons (18) and BPH dox can oxygenate various PCB analogs (4, 7, 16). Details about the structural features which are responsible for the enzyme's substrate recognition, binding, and orientation in the direction of the active site will help us to design new enzymes able to use a broader range of substrates than that currently used.

BPH dox has been studied from *Comamonas testosteroni* B-356 (13, 14) and from *Pseudomonas* sp. strain LB400 (11, 12). It comprises three components (11, 13, 14). These are the terminal oxygenase, an iron-sulfur protein (ISP_{BPH}) made up of an α subunit (M_r = 51,000) and a β subunit (M_r = 22,000), a ferredoxin (FER_{BPH}; M_r = 12,000), and a ferredoxin reductase (RED_{BPH}; M_r = 43,000). The genes that code for these components in both strain B-356 and strain LB400 are *bphA* (ISP_{BPH} α subunit), *bphE* (ISP_{BPH} β subunit), *bphF* (FER_{BPH}), and *bphG* (RED_{BPH}) (6, 31). BPH dox hydroxylates adjacent *ortho-meta* carbons of one of the biphenyl rings to generate 2,3-dihydro-2,3-dihydroxybiphenyl. FER_{BPH} and RED_{BPH} are involved in electron transfer from NADH to ISP_{BPH} (14). One common feature characterizing the terminal oxygenase components of all aromatic ring-hydroxylating dioxygenases is the presence of a [2Fe-2S] Rieske center located on the α subunit (13, 25, 31), which is believed to be involved in electron transfer from the ferredoxin component to a mononuclear Fe^{2+}, which activates molecular oxygen for insertion into the substrate (3, 23). Evidence suggests that the mononuclear Fe^{2+} is coordinated from a domain of the ISP_{BPH} α subunit (15). Therefore, the α subunit appears to serve a major catalytic function. However, the function of the β subunit in enzyme activity has yet to be elucidated.

Purified active ISP_{BPH} preparations were obtained from *Pseudomonas* sp. strain LB400 (11) and from *C. testosteroni* B-356 (14), whereas B-356 RED_{BPH} and FER_{BPH} were purified from *Escherichia coli* recombinant clones as active His-tagged (H-t) proteins (14). Active preparations of H-t B-356 ISP_{BPH} were also obtained (13).

Pseudomonas sp. strain LB400 is one of the best-performing PCB-degrading gram-negative bacteria. An important feature that distinguishes strain LB400 from other PCB degraders is its capacity to catalyze the oxygenation of adjacent *meta-para* carbons of congeners such as 2,2′,5,5′-tetrachlorobiphenyl, in which there are no free adjacent *ortho-meta* carbons (4). Furthermore, strain LB400 metabolizes the double-*ortho*-substituted congener 2,2′-dichlorobiphenyl very efficiently whereas the double-*meta*- or -*para*-substituted congeners such as 3,3′- and 4,4′-dichlorobiphenyl are degraded poorly (4, 7, 10). In spite of the fact that the deduced amino acid sequences of the

* Corresponding author. Mailing address: INRS-Santé, 245 boul. Hymus, Pointe-Claire, Québec, H9R 1G6 Canada. Phone: (514) 630-8829. Fax: (514) 630-8850. E-mail: michel.sylvestre@inrs-sante.uquebec.ca.

LB400 and *Pseudomonas pseudoalcaligenes* KF707 *bphA*, *bphE*, *bphF*, and *bphG* gene products show 95.5, 99.5, 100, and 100% identity, respectively, KF707 BPH dox is unable to attack 2,2′,5,5′-tetrachlorobiphenyl (7, 10, 17). In addition, it poorly metabolizes the double-*ortho*-substituted congener and, unlike strain LB400, it degrades the double-*para*-substituted 4,4′-dichlorobiphenyl more efficiently. Results of recent investigations suggest that a relatively small number of amino acid residues of the carboxy-terminal portion of the ISP_{BPH} α subunit control the substrate selectivity patterns of both strains and their ability to catalyze *meta-para* dioxygenation (7, 17, 24). However, because the ISP_{BPH} β subunits of the two strains used in this study differed by a single amino acid residue, it was impossible to determine any involvement of the β subunit in substrate selectivity.

Strain B-356 BPH dox has unique structural features that distinguish it from strain LB400 BPH dox (the amino acid sequences of the LB400 and B-356 ISP_{BPH} α and β subunits show 76 and 70% identity, respectively) (31). Furthermore, unlike strain LB400, strain B-356 metabolized the double-*meta*-substituted congener 3,3′-dichlorobiphenyl more efficiently than 2,2′- and 4,4′-dichlorobiphenyl. When tested as a resting-cell preparation in a 1-ml volume, 2.4 mg of the 3.3 mg of 3,3′-dichlorobiphenyl was degraded within 12 h, compared to 0.6 and 0.17 mg of 4,4′- and 2,2′-dichlorobiphenyl, respectively (2). In addition, B-356 was unable to degrade 2,2′,5,5′-tetrachlorobiphenyl (2).

Because the recombinant H-t components of B-356 BPH dox have retained all major biochemical features of the parental proteins, affinity chromatography of tagged protein was proposed as a useful tool for examining features of various purified aryl dioxygenase components (13). It especially offers the possibility of comparing the characteristics of purified reconstituted chimeric ISP_{BPH}s, comprised of α and β subunits derived from distinct parent enzymes. In this work we examine the reactivity pattern of BPH dox toward various PCBs and its capacity to catalyze the *meta-para* dioxygenation of chimeric enzymes obtained by exchanging the ISP_{BPH} α or β subunit of strain LB400 with the corresponding subunit of strain B-356. Results show that the structure of the β subunit influences both the capacity of the enzyme to catalyze the *meta-para* oxygenation of the substrate and its substrate reactivity pattern toward PCBs.

MATERIALS AND METHODS

Bacterial strains, culture media, and general protocols. The bacterial strains used in this study were *E. coli* M15(pREP4) and SG13009(pREP4) (both from Qiagen, Inc., Chatsworth, Calif.), *E. coli* SG13009 cured of pREP4 (obtained during this work), *C. testosteroni* B-356 (1), and *Pseudomonas* sp. strain LB400 (4) (also referred as *Burkholderia* sp. strain LB400 or *Pseudomonas cepacia* LB400 [17]). The media used were Luria-Bertani broth (26), H-plate medium (26), and MM30 (29). The plasmids used were pQE31 and pQE51 (Qiagen, Inc.) and pYH31 (to be described elsewhere), which is a new P15A-based plasmid obtained by introducing the operator and promoter region of pQE31, the six-His fusion gene, and the multiple cloning site of pQE31 into the unique *Hin*dIII site of pREP4. pHY31 is compatible with ColE1-based plasmids.

Plasmid DNA from *E. coli* was obtained and restriction endonuclease reactions, ligations, agarose gel electrophoresis, and transformation of *E. coli* cells were done according to protocols described by Sambrook et al. (26). PCRs were performed with *Pwo* DNA polymerase by following the method recommended by Boehringer Mannheim. DNA sequencing was done from subclones of M13mp18 and M13mp19 with a Pharmacia automated laser fluorescence DNA sequencer. Sequence analysis were performed by the DNA sequencing service at the Institut Armand-Frappier, Laval, Québec, Canada.

Previously described procedures (13, 14, 30) were used to obtain purified preparations of each of the following enzymes from recombinant *E. coli* cells: H-t B-356 FER_{BPH}, H-t B-356 RED_{BPH}, H-t B-356 ISP_{BPH} (which carries the His tag on the α subunit), and H-t B-356 2,3-dihydro-2,3-dihydroxybiphenyl 2,3-dehydrogenase. The only exception was that the *E. coli* cells harboring the recombinant pQE31 plasmids were induced at 25°C instead of 37°C as previously described (13). This modification also applies to the other enzyme purification protocols described below.

The LB400 ISP_{BPH} component that carries a His tag on the α subunit was expressed in *E. coli* M15(pREP4), as was done with B-356 H-t ISP_{BPH} (13). The oligonucleotides used to PCR amplify LB400 *bphAE* from genomic LB400 DNA were based on known DNA nucleotide sequences (6). They were oligonucleotide I (*Bam*HI), 5′-CGGGATCCGATGAGTTCAGCAATCA-3′, and oligonucleotide II (*Hin*dIII), 5′-GAGCCAAGCTTGCTAGAAGAACATGCT-3′. The 1.9-kb DNA fragment containing *bphAE* was cloned into the compatible sites of pQE31. H-t LB400 ISP_{BPH} was purified in the same way as H-t B-356 ISP_{BPH} (13).

Purified H-t LB400 FER_{BPH} was obtained by the protocol described for H-t B-356 FER_{BPH} (14). The oligonucleotides used to amplify LB400 *bphF* from genomic DNA of strain LB400 were oligonucleotide I (*Bam*HI), 5′-GCGGGA TCCGATGAAATTTACCAGAG-3′, and oligonucleotide II (*Hin*dIII), 5′-GCG CCAAGCTTGTCATGGCGCCAGATAC-3′.

The ISP_{BPH} chimera with the α subunit of B-356 and the β subunit of LB400 (the $\alpha_{B\text{-}356}\beta_{LB400}$ chimera) carrying the His tag on the α subunit was expressed in *E. coli* M15(pREP4) and purified by the protocol described for H-t B-356 ISP_{BPH} (13). In order to construct the pQE31 chimera with *bphA* from B-356 and *bphE* from LB400 (pQE31[B-356-*bphA*/LB400-*bphE*]), *bphE* was PCR amplified from LB400 genomic DNA with the following oligonucleotides: oligonucleotide I (*Kpn*I), 5′-CCGGGTACCCATGACAAATCCATCCC-3′, and oligonucleotide II (*Kpn*I), 5′-GGGGTACCCCTAGAAGAACATGCT-3′. The 0.6-kb fragment was cloned at the *Kpn*I site of pQE31[B-356-*bphA*], which has been described previously (13).

All of our pQE31[LB400-*bphA*/B-356-*bphE*] constructs poorly expressed bphE. For this reason, the $\alpha_{LB400}\beta_{B\text{-}356}$ ISP_{BPH} chimera was obtained by expressing each subunit from separate plasmids inside the same cell. A DNA fragment carrying LB400 *bphA* was PCR amplified from LB400 genomic DNA with the following oligonucleotides: oligonucleotide I (*Bam*HI), 5′-CGGGATC CGATGAGTTCAGCAATCA-3′, and oligonucleotide II (*Kpn*I), 5′-GCCGGT ACCTTCCTGCTCAGGGCTTGAGCGTG-3′. The 1.3-kb DNA fragment was cloned into compatible sites of pYH31 to construct pYH31[LB400-*bphA*]. B-356 *bphE* was subcloned from pQE31[*bphE*], which was described previously (13), into pQE51, which is an expression vector without the six-His fused gene. Both plasmids were transformed in *E. coli* SG13009 cured of pREP4. Expression and purification of the enzyme were performed by protocols identical to those described previously.

All constructions were such that the His tail added the same 13 amino acids (MRGSHHHHHHTDP) to the protein at the N-terminal portion. The DNA sequences of the constructions obtained by PCR amplification were analyzed to make certain that no mutations were introduced in the amplified DNA.

Protein characterization. Sodium dodecyl sulfate (SDS)-polyacrylamide gels were developed according to the method of Laemmli (20). Proteins were stained with Coomassie brillant blue (26). Protein concentrations were estimated by the method of Lowry et al. (21) with bovine serum albumin as the standard. The concentrations of H-t ISP_{BPH} and FER_{BPH} preparations were also determined spectrophotometrically. The published ε_{450} of 10,100 M^{-1} cm^{-1} (11) was used to determine the concentration of H-t LB400 ISP_{BPH}, and the published ε_{455} of 8,300 M^{-1} cm^{-1} (13) was used to determine the concentrations of H-t B-356 ISP_{BPH} preparations. The concentrations of both LB400 and B-356 H-t FER_{BPH} preparations were determined with the ε_{460} of 7,455 M^{-1} cm^{-1} established for the Rieske center of B-356 FER_{BPH} (14). The concentrations of $\alpha_{LB400}\beta_{B\text{-}356}$ and $\alpha_{B\text{-}356}\beta_{LB400}$ chimeras were determined with an ε_{455} of 8,300 M^{-1} cm^{-1}. The M_r of native protein was determine by high-performance liquid chromatography (HPLC) as described previously (13).

Monitoring of the enzymes' activities and identification of metabolites. Enzyme assays for BPH dox reactions were performed as described previously (13). A reaction was initiated by adding 100 nmol of biphenyl or of one of the following chlorobiphenyls: 2,2′-, 3,3′-, or 4,4′-dichlorobiphenyl; 2,5-dichlorobiphenyl; and 2,2′,5,5′-tetrachlorobiphenyl (all from ULTRAScientific, Kingstown, R.I.) (added in 2 μl of acetone). The reconstituted LB400 H-t BPH dox comprised H-t LB400 ISP_{BPH} plus H-t LB400 FER_{BPH} and H-t B-356 RED_{BPH}; the reconstituted B-356 BPH dox comprised H-t B-356 ISP_{BPH} plus H-t B-356 FER_{BPH} and H-t B-356 RED_{BPH}. Catalytic oxygenation was evaluated by monitoring substrate depletion by HPLC analysis as described previously (13), except that the UV detector of the Hewlett-Packard series 1050 HPLC was set at 203 nm. The K_m and maximal rate of metabolism (V_{max}) for biphenyl was obtained as described previously (13). The catalytic oxygenation of PCBs was evaluated by monitoring substrate depletion 5 min after initiation of the reaction when 100 nmol of substrate was added to initiate the reaction. The metabolites were detected with a Perkin-Elmer LC95 UV- and visible-light detector set at the maximal wavelength established by Haddock et al. (12). Purification of metabolites was as previously described (13, 30). The 2,3-dihydro-2,3-dihydroxybiphenyl 2,3-dehydrogenase assay was performed as previously described (30). The 3,4-dihydroxybiphenyl used as the standard was from ULTRAScientific. Metabolites were identified by gas chromatographic-mass spectrometric (GC-MS) analysis of their trimethylsilyl (TMS) or butylboronate derivatives, using protocols described previously (14, 27). All values reported in the present study are averages of the results of triplicate experiments for at least two distinct enzyme preparations.

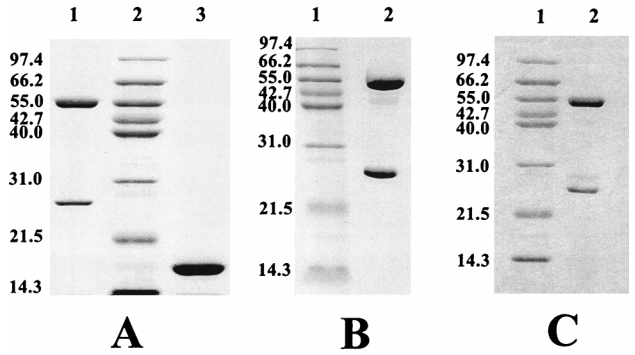

FIG. 1. SDS-PAGE of purified preparations of BPH dox components. (A) Lane 1, preparation of H-t LB400 ISP_{BPH} (3 μg); lane 2, M_r markers; lane 3, preparation of H-t LB400 FER_{BPH} (5 μg); (B) lane 1, M_r markers; lane 2, preparation of the H-t $\alpha_{B\text{-}356}\beta_{LB400}$ ISP_{BPH} hybrid (2.5 μg); (C) lane 1, M_r markers; lane 2, preparation of the H-t $\alpha_{LB400}\beta_{B\text{-}356}$ ISP_{BPH} hybrid (3 μg). Molecular weights (in thousands) are noted at the left sides of the gels.

Site-directed mutagenesis at position Thr-375 of the strain B-356 ISP_{BPH} α subunit. Site-directed mutagenesis was carried out with Pharmacia Biotech's unique site elimination mutagenesis kit, according to the protocol described by Wang and Sul (32). The original sequence of the strain B-356 ISP_{BPH} α subunit, 5′-GC TTG CAG AAG ATC CGC **ACC** TTT AAC GCC GGC GGC-3′, was modified to 5′-GC TTG CAG AAG ATC CGC **AAC** TTT AAC GCC GGC GGC-3′ by replacing Thr-375 with Asn-375 (boldface). Successful mutations were identified by DNA sequencing. Mutant genes were cloned in pQE31. The mutant enzyme was expressed in *E. coli* M15 and purified as fused H-t protein according to protocols described previously (13).

RESULTS

Characterization of H-t LB400 ISP_{BPH} and LB400-B-356 ISP_{BPH} chimeras. Purified H-t LB400 ISP_{BPH} was obtained as described in Materials and Methods. SDS-polyacrylamide gel electrophoresis (PAGE) of the purified preparation showed two single peptide bands with M_rs corresponding to those of the H-t α and β subunits of the LB400 ISP_{BPH} component (Fig. 1A). SDS-PAGE of H-t LB400 FER_{BPH} preparations showed a single band of the expected M_r (Fig. 1A).

The recombinant chimeric H-t ISP_{BPH} preparations used in this study were produced in vivo in *E. coli* clones. H-t $\alpha_{B\text{-}356}$ β_{LB400} ISP_{BPH} was produced in an *E. coli* clone carrying chimeric pQE31[B-356-*bphA*/LB400-*bphE*], whereas H-t $\alpha_{LB400}\beta_{B\text{-}356}$ ISP_{BPH} was produced in an *E. coli* clone carrying pYH31 [LB400-*bphA*] and pQE51[B-356-*bphE*] together. For the latter chimeric protein, SDS-PAGE analysis of the protein eluted from the Ni-nitrilotriacetic acid resin at a low concentration of imidazole combined with densitometric measurement of bands showed that negligible amounts of the ISP_{BPH} β subunit produced inside the cell did not assemble with the α subunit (not shown). Therefore, in spite of the fact that both subunits of H-t $\alpha_{LB400}\beta_{B\text{-}356}$ ISP_{BPH} were expressed from genes located on separate plasmids, the enzyme was effectively reconstituted inside the cell. Purified preparations of both chimeras showed two major bands corresponding to the H-t α and the β subunits (Fig. 1B and C).

HPLC analysis showed that the native conformation of both H-t ISP_{BPH} chimeras was $\alpha_3\beta_3$, as was shown previously for LB400 and B-356 ISP_{BPH} (11, 13). Although we previously reported that types of subunit associations other than that of the $\alpha_3\beta_3$ conformation were detected in some purified preparations of B-356 H-t ISP_{BPH} (13), in the course of the present study we found that when the concentrations of the purified recombinant enzyme preparations were above 100 μM, the $\alpha_3\beta_3$ structure remained intact for all H-t ISP_{BPH} preparations.

As with the parental ISP_{BPH} preparations, the spectral features of both chimeric enzyme preparations were typical of a [2Fe-2S] Rieske-type protein showing maxima at 323 and 455 nm and a shoulder at about 575 nm (not shown). The enzymes were active, and they both catalyzed the oxygenation of biphenyl in the reconstituted BPH dox system.

A K_m value of 103 ± 17 μM and a V_{max} of 1 ± 0.05 nmol of substrate converted per min per μg of ISP_{BPH} (means ± standard deviations) were obtained when H-t LB400 BPH dox composed of H-t LB400 ISP_{BPH}, H-t LB400 FER_{BPH}, and H-t B-356 RED_{BPH} was used to catalyze the dioxygenation of biphenyl. These values are close to those reported for H-t B-356 BPH dox (13). Kinetic parameters of the reconstituted H-t BPH dox comprised of H-t LB400 ISP_{BPH} with H-t LB400 FER_{BPH} were identical to those of the reconstituted enzyme when H-t LB400 FER_{BPH} was replaced by H-t B-356 FER_{BPH}. Similar results were obtained when B-356 ISP_{BPH} was used in combination with H-t LB400 FER_{BPH} or H-t B-356 FER_{BPH}. Therefore, both FER_{BPH}s can be interchanged with no effect on activity. Similar K_m (66 ± 9 μM) and V_{max} (0.6 ± 0.02 nmol/min/μg of ISP_{BPH}) values were obtained for the H-t chimeric BPH dox composed of H-t $\alpha_{B\text{-}356}\beta_{LB400}$ ISP_{BPH}, H-t B-356 FER_{BPH}, and H-t B-356 RED_{BPH}. The reconstituted H-t chimeric α_{LB400} $\beta_{B\text{-}356}$ ISP_{BPH} was also functional, but its K_m value towards biphenyl was slightly higher (K_m = 370 ± 65 μM; V_{max} = 0.9 ± 0.04 nmol/min/μg of ISP_{BPH}).

Reactivities of reconstituted purified H-t LB400 dox and H-t B-356 BPH dox and of H-t LB400–B-356 BPH dox chimeras toward selected PCBs. In a previous study, when biphenyl was used as the substrate, the TMS-derived diol products of the B-356 BPH dox reaction were resolved into two distinct peaks by GC-MS analysis. These two peaks were postulated to be 2,3-dihydro-2,3-dihydroxybiphenyl and 3,4-dihydro-3,4-dihydroxybiphenyl, respectively (14). However, it was later found that when *n*-butylboronate was used for chemical derivatization of biphenyl metabolites, a single GC-MS peak was obtained. Moreover, the biphenyl-derived dihydrodiol product of the B-356 BPH dox reaction eluted as a single HPLC peak (30). The TMS-derived dihydrodiol obtained from this HPLC peak was resolved as two GC-MS peaks (results not shown). However, when the HPLC-purified 2,3-dihydro-2,3-dihydroxybiphenyl was used as the substrate for the 2,3-dihydro-2,3-dihydroxybiphenyl 2,3-dehydrogenase reaction, both of these TMS-derived dihydrodiol peaks disappeared from the reaction medium and 2,3-dihydroxybiphenyl was the unique metabolite generated in this reaction (results not shown). 3,4-Dihydroxybiphenyl was not produced. Therefore, the resolution of the TMS-derived dihydrodiol into two GC-MS peaks is an artifact. Although at this time we cannot provide an explanation for this artifact, the data presented above clearly show that our former assumption that B-356 BPH dox can catalyze a *meta-para* hydroxylation of biphenyl was erroneous.

Two other observations supported the inability of B-356 BPH dox to catalyze the *meta-para* hydroxylation reaction. When *n*-butylboronate was used for chemical derivatization of the metabolites obtained from 2,5-dichlorobiphenyl, a single dihydrodiol was detected by GC-MS from the B-356 BPH dox reaction whereas two *n*-butylboronate-derived dihydrodiol metabolites were detected from LB400 BPH dox reaction media. The retention time and mass spectral features of the single dihydrodiol metabolite produced by B-356 BPH dox were identical to those of the major metabolite produced by LB400 BPH dox (Fig. 2). This metabolite must be the 2′,3′-dihydro-2′,3′-dihydroxy-2,5-dichlorobiphenyl which has previously been identified by nuclear magnetic resonance as the major metabolite produced from 2,5-dichlorobiphenyl by LB400 BPH dox

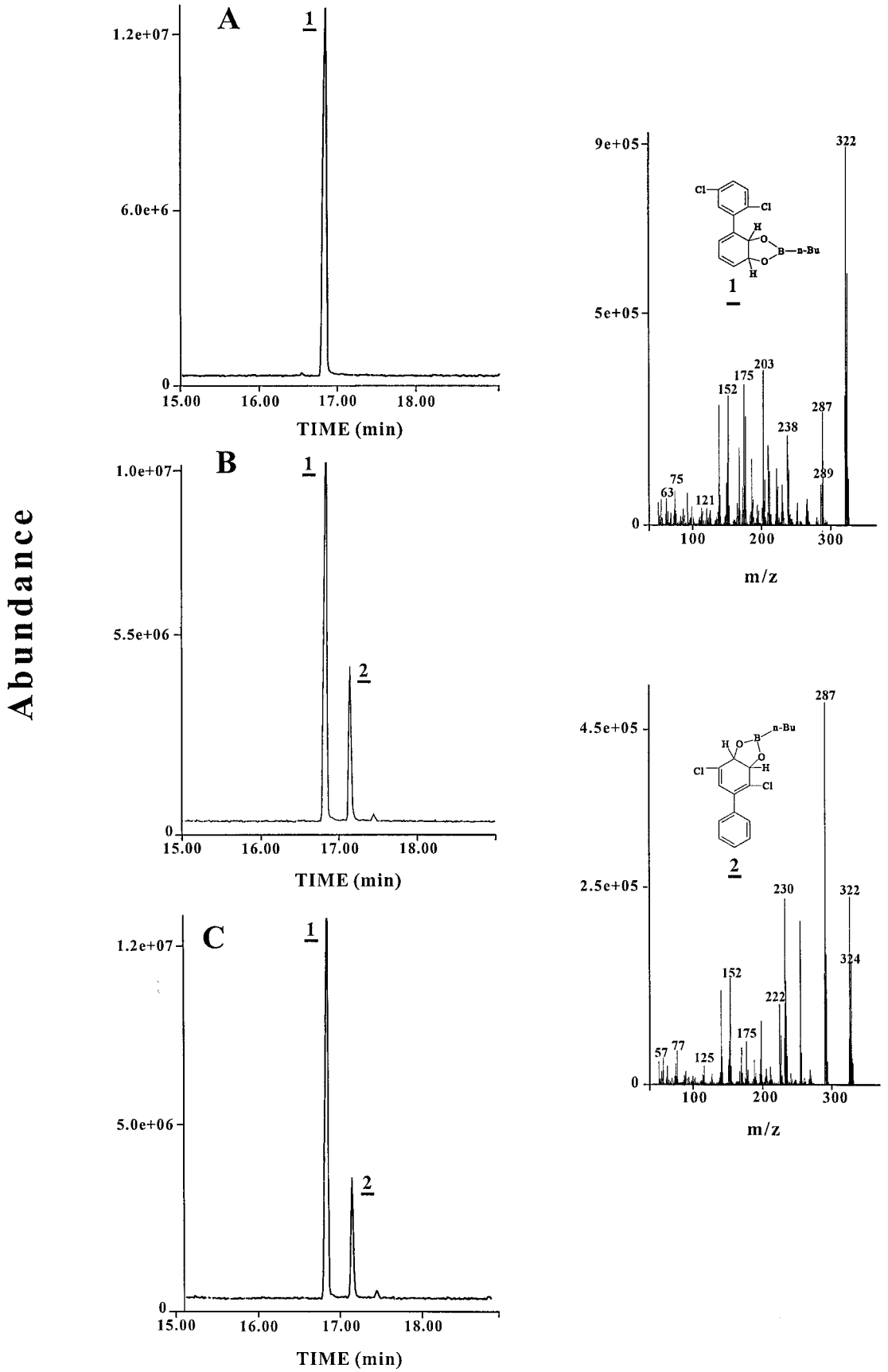

FIG. 2. GC-MS spectra of the butylboronate-derived metabolites obtained from 2,5-dichlorobiphenyl when the substrate was oxygenated with B-356 H-t BPH dox (A), LB400 H-t BPH dox (B), or H-t $\alpha_{B\text{-}356}\beta_{LB400}$ BPH dox (C). n-Bu, *n*-butylboronate.

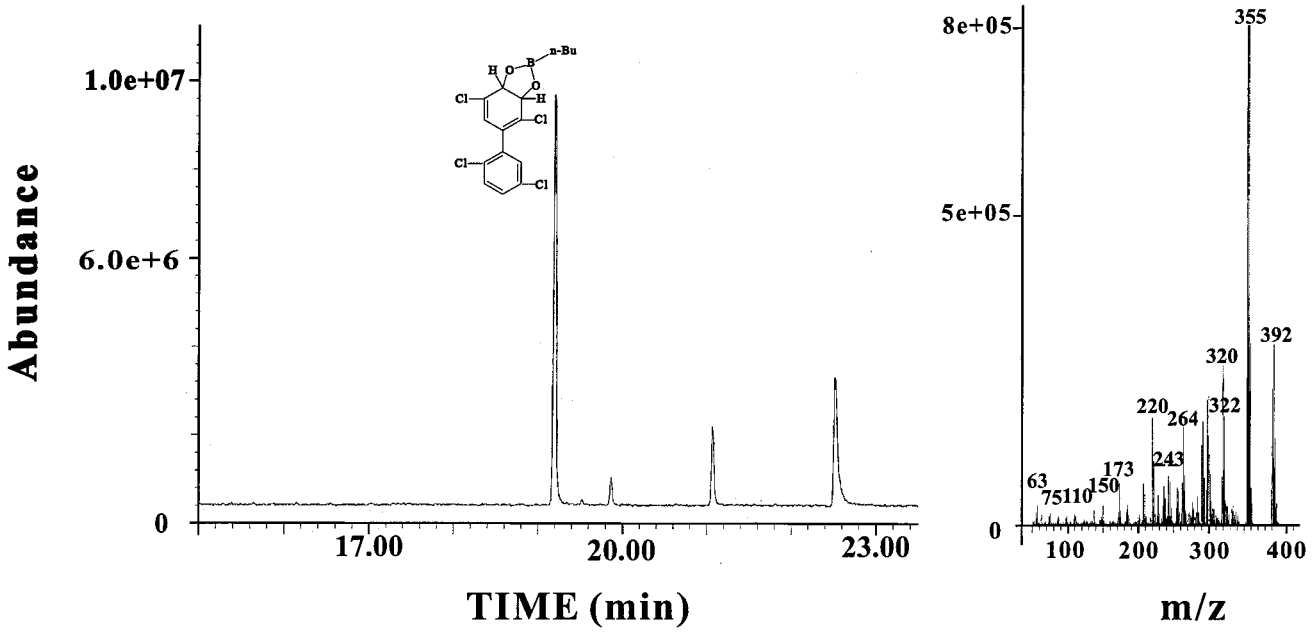

FIG. 3. GC-MS spectra of the dihydrodiol metabolite produced from 2,2′,5,5′-tetrachlorobiphenyl when H-t $\alpha_{B\text{-}356}\beta_{LB400}$ ISP_{BPH} was used to reconstitute BPH dox. n-Bu, *n*-butylboronate.

(12). The minor metabolite produced by LB400 BPH dox had tentatively been identified as the product resulting from the *meta-para* oxygenation of the molecule (12), and this metabolite was not produced in the B-356 BPH dox reaction mixture (Fig. 2).

Furthermore, no dihydrodiol metabolite was detected by GC-MS and by HPLC analyses when 2,2′,5,5′-tetrachlorobiphenyl was supplied as the substrate for the H-t B-356 BPH dox reaction. Conversely, as expected from a previous report (12), the corresponding 3,4-dihydrodiol metabolite was produced in a large amount when this reaction was catalyzed by H-t LB400 BPH dox.

It is noteworthy that the metabolites produced from 2,5-dichlorobiphenyl when H-t $\alpha_{B\text{-}356}\beta_{LB400}$ ISP_{BPH} was used to reconstitute BPH dox were the same as those generated by LB400 H-t ISP_{BPH} (Fig. 2). Furthermore, 2,2′,5,5′-tetrachlorobiphenyl was metabolized to the 3,4-dihydro-3,4-dihydroxy-2,2′,5,5′-tetrachlorobiphenyl (Fig. 3) by this chimeric enzyme. 3,4-Dihydro-3,4,-dihydroxy-2,2′,5,5′-tetrachlorobiphenyl was also produced from 2,2′,5,5′-tetrachlorobiphenyl by the H-t $\alpha_{LB400}\beta_{B\text{-}356}$ ISP_{BPH} chimera (not shown). However, as seen below, the rate of transformation was not as high as for the H-t $\alpha_{B\text{-}356}\beta_{LB400}$ ISP_{BPH} hybrid. If the α subunit were the sole determinant controlling the capacity of the enzyme to catalyze a *meta-para* oxygenation, $\alpha_{B\text{-}356}\beta_{LB400}$ ISP_{BPH} should not have metabolized 2,2′,5,5′-tetrachlorobiphenyl. Thus, considered together, these data show that the capacity of the enzyme to catalyze a *meta-para* hydroxylation of selected congeners is largely determined by the overall enzyme structure imposed by the association between the α and β subunits.

In previous investigations (4, 7, 10) LB400 BPH dox was found to metabolize efficiently 2,2′-dichlorobiphenyl but to metabolize poorly 3,3′- and 4,4′-dichlorobiphenyl whereas strain B-356 was found to preferentially metabolize 3,3′-dichlorobiphenyl. It was thus convenient to use these three dichlorinated congeners to compare the substrate preferences of the parental and chimeric enzymes.

It was virtually impossible to obtain statistically significant values to determine the kinetic parameters of these substrates because their water solubility is very low (5, 8, 22), they are degraded very slowly by the enzyme, and some of their enzyme components lose their activity within a few minutes after initiation of the reaction. Instead, we have determined the activities of the various enzyme preparations toward PCB congeners by evaluating their degradation over a period of 5 min.

Data shown in Table 1 confirmed the preference of LB400

TABLE 1. Amounts of substrate depleted 5 min after initiation of reactions with the indicated enzymes[a]

Substrate	nmol of substrate depleted/0.6 nmol of enzyme:			
	$\alpha_{B\text{-}356}\beta_{B\text{-}356}$ ISP_{BPH}	$\alpha_{LB400}\beta_{LB400}$ ISP_{BPH}	$\alpha_{B\text{-}356}\beta_{LB400}$ ISP_{BPH}	$\alpha_{LB400}\beta_{B\text{-}356}$ ISP_{BPH}
2,2′-Dichlorobiphenyl	<10	50	50	30
3,3′-Dichlorobiphenyl	50	<10	<10	30
4,4′-Dichlorobiphenyl	T	T	T	T
2,5-Dichlorobiphenyl	50	60	30	<10
2,2′,5,5′-Tetrachlorobiphenyl	−	35	40	20

[a] BPH dox reactions were carried out as described in Materials and Methods. Substrate (100 nmol) was added to initiate each reaction. Numbers refer to the amounts of substrate consumed 5 min after initiation of the reactions. The values are averages of results from three separate experiments with two different enzyme preparations. The variance was less than 10% in all cases. −, no degradation; T, trace amounts of metabolite produced.

BPH dox for 2,2′-dichlorobiphenyl (24). Product analysis showed that 3,3′- and 4,4′-dichlorobiphenyl were metabolized to dihydrodiol derivatives. However, the rate of transformation was extremely low. In fact, less than 5 nmol of these substrates was depleted from the reaction medium when the reaction was prolonged for 10 min. On the other hand, under the same conditions B-356 BPH dox metabolized 3,3′-dichlorobiphenyl much faster than 2,2′- and 4,4′-dichlorobiphenyl, which also confirmed previously reported results (2). It is noteworthy that when the reaction was catalyzed by the H-t $\alpha_{B\text{-}356}\beta_{LB400}$ ISP_{BPH} hybrid, the reactivity pattern was similar to that of H-t LB400 BPH dox. The H-t BPH dox $\alpha_{LB400}\beta_{B\text{-}356}$ chimera has acquired features of both parents. It transformed both 2,2′- and 3,3′-dichlorobiphenyl at comparable rates (Table 1). Similar to the observation made when 2,2′,5,5′-tetrachlorobiphenyl was used as a substrate, data showed that the α subunit is not the sole determinant of the enzyme's reactivity pattern toward the dichlorinated congeners. Thus, the substrate metabolization pattern of $\alpha_{B\text{-}356}\beta_{LB400}$ ISP_{BPH} is similar to that of LB400 ISP_{BPH} instead of B-356 ISP_{BPH}. On the other hand, the $\alpha_{LB400}\beta_{B\text{-}356}$ chimera transformed 2,2′,5,5′-tetrachlorobiphenyl less efficiently than the $\alpha_{B\text{-}356}\beta_{LB400}$ chimera.

Site-directed mutagenesis at position Thr-375 of the strain B-356 ISP_{BPH} α subunit. Mondello et al. (24) have categorized 15 strains into two groups based on their ability to degrade PCB congeners. One group (LB400 type) showed a broad range of congener specificity, including the capacity to degrade 2,2′,5,5′-tetrachlorobiphenyl, whereas the second group (KF707 type) showed a much narrower range of PCB congener specificity. Sequence comparison between the ISP_{BPH} α subunits of these two groups identified four regions of the protein C-terminal portion in which specific sequences were consistently associated with either broad or narrow substrate specificity (24). Strain B-356 fits in with the KF707-type strains. It shows a narrow congener substrate specificity. It poorly degrades 2,2′-dichlorobiphenyl, and it is unable to catalyze the *meta-para* hydroxylation of 2,2′,5,5′-tetrachlorobiphenyl. Furthermore, the amino acid residues of all four regions identified by Mondello et al. (24) as being involved in determining substrate specificity are identical to the residues found in the KF707-type strains (Fig. 4). Moreover, among the residues that are not conserved in all the sequences shown in Fig. 4, 42 residues found in the B-356 ISP_{BPH} α subunit are also found in the KF707-type ISP_{BPH}, compared with only 4 residues found in the LB400 type.

In a previous investigation, site-directed mutagenesis of the KF707 ISP_{BPH} α subunit at Thr-376 (KF707) (region IV) to Asn-376 (as in LB400) (17) resulted in the expansion of the range of biodegradable PCB congeners, including those requiring a *meta-para* dioxygenation of the molecule. Furthermore, a combination of mutations at regions III and IV of the LB400 ISP_{BPH} α subunit showed that replacing Asn-377 by Thr-377 (as in KF707) strongly hindered the capacity of the enzyme to catalyze the oxygenation of 2,2′,5,5′-tetrachlorobiphenyl when the amino acid sequence of region III was identical to the one found in the KF707 ISP_{BPH} α subunit. Region III of the B-356 ISP_{BPH} α subunit is very similar to that of KF707, except that Ala-336 of KF707 is replaced in B-356 by Gly-335, which is of similar hydrophobicity (19, 33). Therefore, it was interesting to evaluate the effect of changing Thr-375 of the B-356 ISP_{BPH} α subunit to Asn-375 as in LB400. Based on the investigations cited above, the mutant enzyme was expected to catalyze *meta-para* hydroxylations. However, when the purified H-t mutant enzyme was assayed with 2,5-dichlorobiphenyl as the substrate, HPLC and GC-MS analyses of the reaction product showed that 2′,3′-dihydro-2′,3′-dihydroxy-2,5-dichlorobiphenyl was the unique metabolite of this reaction (not shown). Furthermore, this mutant was unable to transform 2,2′,5,5′-tetrachlorobiphenyl. Therefore, in spite of the strong structural similarity of designated regions between KF707 and B-356 ISP_{BPH} α subunits, the structural features of the ISP_{BPH} α subunit C-terminal portion that were found to strongly influence KF707 and LB400 BPH dox activity did not influence the substrate reactivity pattern of B-356 BPH dox. Altogether, our data show that other structural features, some of which are associated with the β subunit, also influence enzyme activity toward PCB congeners.

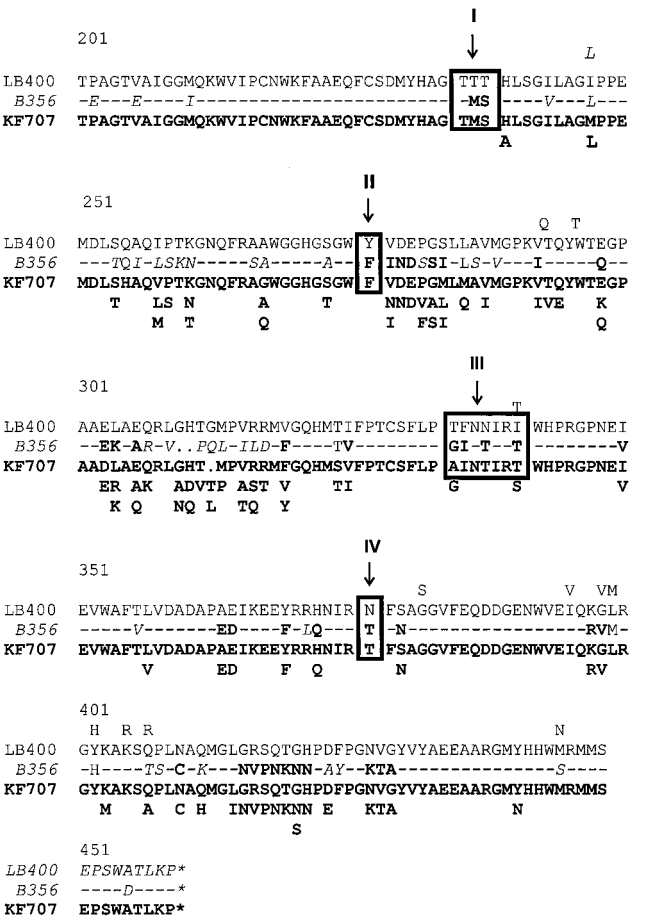

FIG. 4. Sequence comparison between the C-terminal portion of the B-356 ISP_{BPH} α subunit with those of KF707- and LB400-type ISP_{BPH}s. Regions I, II, III, and IV are those designated by Mondello et al. (24). Residues above the LB400 sequence are, according to the work of Mondello et al. (24), residues found at these positions in other LB400-type ISP_{BPH}s; residues below the KF707 sequence are those found at these positions in other KF707-type ISP_{BPH}s. Dashes represent residues that are conserved in all three sequences. Residues of B-356 ISP_{BPH} in boldface type are found in KF707-type ISP_{BPH}s; those in lightface type are found in LB400-type ISP_{BPH}s. Characters in italics are either found in both types or differ from both types.

DISCUSSION

In this study we have engineered novel ISP_{BPH} hybrids by replacing the B-356 ISP_{BPH} α or β subunit with the corresponding polypeptide recruited from strain LB400 BPH dox. The ISP_{BPH} chimeras representing the two associations (the $\alpha_{LB400}\beta_{B\text{-}356}$ and $\alpha_{B\text{-}356}\beta_{LB400}$ chimeras) were functional.

When the catalytic activities towards various PCBs of the

novel chimeric enzymes were compared to those of the parent enzymes, results showed that the structure of the ISP_{BPH} β subunit influences the reactivity pattern of the enzymes as well as their capacity to catalyze the oxygenation of the *meta-para* carbons. At first glance, these results appear to contradict those obtained by Mondello et al. (24) and Kimura et al. (17), who found that only a small number of amino acid residues located in the carboxy-terminal halves of the KF707 and LB400 ISP_{BPH} α subunits control the enzymes' reactivities toward PCB congeners. However, it is noteworthy that these studies were carried out with two very closely related dioxygenases. The sequences of the β subunits for LB400 and KF707 ISP_{BPH} differ by a single amino acid residue (7). In the present study, by using two more distantly related BPH doxes, it was possible to show an influence of the structure of the β subunit on the enzyme reactivity pattern. Furthermore, data obtained with the LB400–B-356 chimeric enzymes show that the amino acid residues of the LB400 and KF707 α subunits, which were found in previous investigations to greatly influence the substrate reactivity patterns of LB400 and KF707 BPH dox, did not appear to influence the reactivity patterns of B-356 BPH dox and of LB400–B-356 BPH dox chimeras.

By changing amino acids 335 to 341 (Thr-Phe-Asn-Asn-Ile-Arg-Ile [region III]) of the *Pseudomonas* sp. strain LB400 ISP_{BPH} α subunit to the sequence Ala-Ile-Asn-Thr-Ile-Arg-Thr as in the *P. pseudoalcaligenes* KF707 ISP_{BPH} α subunit, Erickson and Mondello (7) obtained mutants which were able to efficiently metabolize the otherwise poorly degraded substrate 4,4′-dichlorobiphenyl, thus broadening the enzyme's substrate reactivity.

As noticed above, the region III amino acid sequence of the strain B-356 ISP_{BPH} α subunit differs from that of strain KF707 by a single amino acid residue (Fig. 4). Yet, unlike the enzyme of strain KF707, both strain B-356 BPH dox and the chimeric enzyme $\alpha_{B\text{-}356}\beta_{LB400}$ ISP_{BPH} poorly metabolize 4,4′-dichlorobiphenyl.

Similarly, changing simultaneously Asn-377 and Phe-336 of the LB400 ISP_{BPH} α subunit to Thr-377 and Ile-336 (as in the KF707 α subunit) drastically reduced the capacity of the mutant to catalyze the *meta-para* oxygenation of the molecule (24). Changing Thr-376 of the KF707 ISP_{BPH} α subunit to Asn-376, as in LB400, resulted in an expansion of the range of biodegradable congeners, including those requiring a *meta-para* attack. However, although the corresponding position is occupied by a Thr in the strain B-356 α subunit, $\alpha_{B\text{-}356}\beta_{LB400}$ ISP_{BPH}, unlike KF707 ISP_{BPH}, can transform 2,2′,5,5′-tetrachlorobiphenyl into the 3,4-dihydro-3,4-dihydroxychlorobiphenyl derivative. Furthermore, changing Thr-375 of the B-356 ISP_{BPH} α subunit to Asn-375, as in LB400, did not confer to the mutant the capacity to oxygenate 2,5-dichlorobiphenyl onto *meta-para* carbons.

Finally, the fact that the substrate selectivity pattern of the $\alpha_{LB400}\beta_{B\text{-}356}$ chimera differs from that of LB400 and of B-356 BPH dox is further evidence that the structures of both subunits influence the substrate selectivity of the enzyme.

Our data are insufficient to precisely determine the function of the β subunit in BPH dox activity. However, for the first time, we provide clear evidence with purified enzyme preparations that both the α and β subunits of the aryl-hydroxylating dioxygenases influence the enzyme-substrate interaction. The amino acid residues of the α subunit that affect enzyme reactivity in one type of α-β arrangements, that of the $\alpha_{LB400}\beta_{LB400}$ arrangement, have no effect on other types of α-β arrangements, such as that of the $\alpha_{B\text{-}356}\beta_{LB400}$ chimera. To explain these results, it is likely that a catalytic poach is created by the association between the α and β subunits. Structural features of both subunits would then influence the dimension and shape of the catalytic poach to determine which PCBs can be oxygenated as well as the orientations of the adjacent reactive carbons toward the active site. This observation is important in terms of engineering enzymes to increase the range of the catalytic activities toward PCBs. Current investigation in our laboratory aims at identifying the residues of both the large and small ISP_{BPH} subunits which are involved subunit association as well as substrate binding and orientation in the direction of the enzyme's active site.

ACKNOWLEDGMENT

This work was supported by grant STP0193182 from the Natural Sciences and Engineering Research Council of Canada.

REFERENCES

1. **Ahmad, D., R. Massé, and M. Sylvestre.** 1990. Cloning and expression of genes involved in 4-chlorobiphenyl transformation by *Pseudomonas testosteroni* strain B-356: homology to polychlorobiphenyl-degrading genes in other bacteria. Gene **86:**53–61.
2. **Barriault, D., C. Pelletier, Y. Hurtubise, and M. Sylvestre.** 1997. Substrate-selectivity pattern of *Comamonas testosteroni* B-356 towards dichlorobiphenyls. Int. Biodeterior. Biodegrad. **39:**311–316.
3. **Batie, C. J., D. P. Ballou, and C. J. Correll.** 1991. Phatalte dioxygenase reductase and related flavin-iron-sulfur containing electron transferases, p. 544–554. *In* F. Müller (ed.), Chemistry and biochemistry of flavoenzymes. CRC Press, Boca Raton, Fla.
4. **Bedard, D. L., R. Unterman, L. H. Bopp, M. J. Brennan, M. L. Haberl, and C. Johnson.** 1986. Rapid assay for screening and characterizing microorganisms for the ability to degrade polychlorinated biphenyls. Appl. Environ. Microbiol. **51:**761–768.
5. **Dulfer, W. J., and H. A. J. Grovers.** 1995. Solubility and micell-water partitioning of polychlorinated biphenyls in solutions of bile salt micelles. Chemosphere **30:**293–306.
6. **Erickson, B. D., and F. J. Mondello.** 1992. Nucleotide sequencing and transcriptional mapping of the genes encoding biphenyl dioxygenase, a multicomponent polychlorinated-biphenyl-degrading enzyme in *Pseudomonas* strain LB400. J. Bacteriol. **174:**2903–2912.
7. **Erickson, B. D., and F. J. Mondello.** 1993. Enhanced biodegradation of polychlorinated biphenyl after site-directed mutagenesis of a biphenyl dioxygenase gene. Appl. Environ. Microbiol. **59:**3858–3862.
8. **Erickson, D. E.** 1986. Analytical chemistry of PCB's. Ann Arbor Science Book, Butterworth, Boston, Mass.
9. **Furukawa, K., S. Hayashida, and K. Taira.** 1992. Biochemical and genetic basis for the degradation of polychlorinated biphenyls in soil bacteria, p. 257–267. *In* E. Galli, S. Silver, and B. Witholt (ed.), *Pseudomonas* molecular biology and biotechnology. American Society for Microbiology, Washington, D.C.
10. **Gibson, D. T., D. L. Cruden, J. D. Haddock, G. J. Zylstra, and J. M. Brand.** 1993. Oxidation of polychlorinated biphenyls by *Pseudomonas* sp. strain LB400 and *Pseudomonas pseudoalcaligenes* KF707. J. Bacteriol. **175:**4561–4564.
11. **Haddock, J. D., and D. T. Gibson.** 1995. Purification and characterization of the oxygenase component of biphenyl 2,3-dioxygenase from *Pseudomonas* sp. strain LB400. J. Bacteriol. **177:**5834–5839.
12. **Haddock, J. D., J. R. Horton, and D. T. Gibson.** 1995. Dihydroxylation and dechlorination of chlorinated biphenyls by purified biphenyl 2,3-dioxygenase from *Pseudomonas* sp. strain LB400. J. Bacteriol. **177:**20–26.
13. **Hurtubise, Y., D. Barriault, and M. Sylvestre.** 1996. Characterization of active recombinant His-tagged oxygenase component of *Comamonas testosteroni* B-356 biphenyl dioxygenase. J. Biol. Chem. **271:**8152–8156.
14. **Hurtubise, Y., D. Barriault, J. Powlowski, and M. Sylvestre.** 1995. Purification and characterization of the *Comamonas testosteroni* B-356 biphenyl dioxygenase components. J. Bacteriol. **177:**6610–6618.
15. **Jiang, H., R. E. Parales, N. A. Lynch, and D. T. Gibson.** 1996. Site-directed mutagenesis of conserved amino acids in the *alpha* subunit of toluene dioxygenase: potential mononuclear non-heme iron coordination sites. J. Bacteriol. **178:**3133–3139.
16. **Kimura, N., H. Kato, N. Akito, and K. Furukawa.** 1996. Analysis of substrate range of biphenyl-catabolic enzymes. Biosci. Biotechnol. Biochem. **60:**220–223.
17. **Kimura, N., A. Nishi, M. Goto, and K. Furukawa.** 1997. Functional analysis of a variety of chimeric dioxygenases constructed from two biphenyl dioxygenases that are similar structurally but different functionally. J. Bacteriol. **179:**3936–3943.
18. **Kiyohara, H., S. Torigoe, N. Kaida, T. Asaki, T. Iida, H. Hayashi, and N. Takizawa.** 1994. Cloning and characterization of a chromosomal gene cluster, *pah*, that encodes the upper pathway for phenanthrene and naphthalene

utilization by *Pseudomonas putida* OUS82. J. Bacteriol. **176:**2439–2443.
19. **Kyte, J., and R. Doolite.** 1982. A simple method for displaying the hydropathic character of a protein. J. Mol. Biol. **157:**105–132.
20. **Laemmli, U. K.** 1970. Cleavage of structural proteins during the assembly of the head of bacteriophage T4. Nature (London) **227:**680–685.
21. **Lowry, O. H., N. J. Rosebrough, A. L. Far, and R. J. Randall.** 1951. Protein measurement with the Folin phenol reagent. J. Biol. Chem. **193:**265–275.
22. **MacKay, D., P. Mascarenhas, and W. Y. Shiu.** 1980. Aqueous solubility of polychlorinated biphenyls. Chemosphere **9:**257–264.
23. **Mason, J. R., and R. Cammack.** 1992. The electron-transport proteins of hydroxylating bacterial dioxygenases. Annu. Rev. Microbiol. **46:**277–305.
24. **Mondello, F. J., M. P. Turcich, J. H. Lobos, and B. D. Erickson.** 1997. Identification and modification of biphenyl dioxygenase sequences that determine the specificity of polychorinated biphenyl degradation. Appl. Environ. Microbiol. **63:**3096–3103.
25. **Neidle, E. L., C. Hartnett, N. Ornston, A. Bairoch, M. Rekik, and S. Harayama.** 1991. Nucleotide sequences of the *Acinetobacter calcoaceticus benABC* genes for benzoate 1,2-dioxygenase reveal evolutionary relationships among multicomponent oxygenases. J. Bacteriol. **173:**5385–5395.
26. **Sambrook, J., E. F. Fritsch, and T. Maniatis.** 1989. Molecular cloning: a laboratory manual, 2nd ed. Cold Spring Harbor Laboratory Press, Cold Spring Harbor, N.Y.
27. **Sondossi, M., M. Sylvestre, and D. Ahmad.** 1992. Effects of chlorobenzoate transformation of the *Pseudomonas testosteroni* biphenyl and chlorobiphenyl degradation pathway. Appl. Environ. Microbiol **58:**485–495.
28. **Sylvestre, M.** 1995. Biphenyl/chlorobiphenyls catabolic pathway of *Comamonas testosteroni* B-356: prospect for use in bioremediation. Int. Biodeterior. Biodegrad. **34:**189–211.
29. **Sylvestre, M., and J. Fauteux.** 1982. A new facultative anaerobe capable of growth on chlorobiphenyls. J. Gen. Appl. Microbiol. **28:**61–72.
30. **Sylvestre, M., Y. Hurtubise, D. Barriault, J. Bergeron, and D. Ahmad.** 1996. Characterization of active recombinant 2,3-dihydro-2,3-dihydroxybiphenyl dehydrogenase from *Comamonas testosteroni* B-356 sequence of the encoding gene (*bphB*). Appl. Environ. Microbiol. **62:**2710–2715.
31. **Sylvestre, M., M. Sirois, Y. Hurtubise, J. Bergeron, D. Ahmad, F. Shareck, A. Larose, D. Barriault, I. Guillemette, and J. M. Juteau.** 1996. Sequencing of *Comamonas testosteroni* strain B-356-biphenyl/chlorobiphenyl dioxygenase genes: evolutionary relationships among Gram-negative biphenyl dioxygenases. Gene **174:**195–202.
32. **Wang, D., and H. S. Sul.** 1996. Site-directed mutagenesis for large insertions by oligonucleotide primers in optimized molar ratios. BioTechniques **22:**70–72.
33. **Wolfenden, R., L. Andersson, P. Cullis, and C. Southgate.** 1981. Affinities of amino acid side chains for solvent water. Biochemistry **20:**849–855.